# Platinum(II) 1,5-COD Oxo Complexes

**Hui Shan, Alan James, and Paul R. Sharp***

Department of Chemistry, University of Missouri—Columbia, Columbia, Missouri 65211

*Received July 14, 1998*

Three new types of platinum(II) oxo complexes—$[(1,5\text{-COD})Pt(\mu^3\text{-O})(AuL)]_2(BF_4)_2$ [**1**, L = $PPh_3$, $PPh_2Et$, $PPh_2$-*i*-Pr, P(*o*-tol)$_3$, P(*p*-tol)$_3$, P(*p*-$MeOC_6H_4$)$_3$, P(*p*-$CF_3C_6H_4$)$_3$], $[(1,5\text{-COD})Pt\{\mu^3\text{-O}(AuL)_2\}_2](BF_4)_2$ (**2**), and $[(1,5\text{-COD})_4Pt_4(\mu^3\text{-O})_2Cl_2]X_2$ (**3**, X = $BF_4$; **3a**, X = $CF_3SO_3$)—are obtained from oxo/chloro exchange reactions between (1,5-COD)$PtCl_2$ and $[(LAu)_3(\mu^3\text{-O})]BF_4$. Crystals of **1** (L = $PPh_3$) from $CDCl_3$ are triclinic, $P\bar{1}$, with (−100 °C) $a$ = 9.187(4) Å, $b$ = 12.149(3) Å, $c$ = 17.680(6) Å, $\alpha$ = 99.58(2)°, $\beta$ = 102.86(2)°, $\gamma$ = 111.63(2)°, $V$ = 1720(1) Å$^3$, and $Z$ = 1. Crystals of **3a** from $CH_2Cl_2$/toluene are trigonal, $P3_121$, with $a$ = 11.8878(4) Å, $c$ = 29.3193(15) Å, $V$ = 3588.3(3) Å$^3$, and $Z$ = 3. The structure of the cationic portion of **1** shows a planar (COD)$Pt(\mu\text{-O})_2$Pt(COD) unit with slightly out-of-plane $LAu^+$ groups linearly coordinated to the oxo ligands. The structure of the cationic portion of **3a** is similar and shows a slightly folded (COD)$Pt(\mu\text{-O})_2$Pt(COD) unit with out-of-plane $[(COD)PtCl]^+$ groups coordinated to the oxo ligands. Solutions of **3** in untreated $CH_2Cl_2$ or $CD_2Cl_2$ deposit crystals of $[(1,5\text{-COD})_4Pt_4(\mu^3\text{-O})_2(\mu^2\text{-OH})](BF_4)_3$ (**4**) which are monoclinic, $P2_1/n$, with $a$ = 18.624(4) Å, $b$ = 14.760(2) Å, $c$ = 15.584(5) Å, $\beta$ = 95.538(12)°, $V$ = 4264(2) Å$^3$, and $Z$ = 4. The core structure of the cationic portion of **4** shows a tetranuclear platinum cation in which the metal atoms occupy the corners of a distorted tetrahedron and two $\mu^3$-oxo ligands and one $\mu^2$-hydroxo ligand bridge the four platinum atoms. Reaction of **1** (L = $PPh_3$) with $PPh_3$ gives $OPPh_3$ and $[(Ph_3P)_3PtAuPPh_3]BF_4$ (**5**) which is also obtained from $(Ph_3P)_4Pt$ and $Ph_3PAuBF_4$. Crystals of **5** from THF are monoclinic, $P2_1/c$, with $a$ = 20.426(6) Å, $b$ = 13.4980(11) Å, $c$ = 24.703(9) Å, $\beta$ = 97.166(15)°, $V$ = 6758(3) Å$^3$, and $Z$ = 4. The structure of **5** consists of an $L_3Pt-AuL$ cation where the Au atom is linear 2-coordinate and the Pt atom is distorted square-planar 4-coordinate.

## Introduction

Current interest in late-transition metal oxygen and nitrogen bonds originates in part from the anticipated high reactivity of these bonds.[1−3] We have been interested in the synthesis and properties of late-transition-metal oxo, imido, and related complexes,[4−7] partly because of the proposed high reactivity and partly as models for surface species in late-transition-metal heterogeneously catalyzed reactions.[8] Our primary synthetic approach to these complexes has been deprotonation of cationic hydroxo and amido complexes with strong bases. Other approaches that do not require such strongly basic conditions are needed to access a greater diversity of complexes. Recently we reported novel oxo-centered Au−Rh clusters formed by oxo/chloro exchange between the gold oxo complexes $[(Ph_3PAu)_3(\mu^3\text{-O})]BF_4$ and $[(diene)Rh(\mu^2\text{-Cl})]_2$ (diene = 1,5-COD, NBD).[6] Exchange reactions of this type offer a mild approach to oxo and imido complexes, and we have worked on expanding these reactions to other metal systems. Here, we report our results with (1,5-COD)$PtCl_2$.

## Results

The product of the reaction of $[(LAu)_3(\mu^3\text{-O})]BF_4$ with (1,5-COD)$PtCl_2$ in THF depends on the reactant ratios (Scheme 1). A 1:1 ratio gives pale yellow-air-stable $[(1,5\text{-COD})Pt(\mu^3\text{-O})(AuL)]_2(BF_4)_2$ [**1**; L = $PPh_3$, $PPh_2Et$, $PPh_2$-*i*-Pr, P(*o*-tol)$_3$, P(*p*-tol)$_3$, P(*p*-$MeOC_6H_4$)$_3$, P(*p*-$CF_3C_6H_4$)$_3$] and LAuCl. The structure of the cationic portion of **1** (L = $PPh_3$), determined by X-ray diffraction, is shown in Figure 1 and consists of a planar (COD)$Pt(\mu\text{-O})_2$Pt(COD) unit with slightly out-of-plane $LAu^+$ groups linearly coordinated to the oxo ligands in an anti orientation. Crystallographic data are given in Table 1, and selected distances and angles are presented in Table 2. $^{31}$P NMR spectra of **1** show a single peak (no $^{195}$Pt coupling) in a shift region near that of parent $[(LAu)_3(\mu^3\text{-O})]BF_4$. $^1$H and $^{13}$C NMR spectra show, in addition to the phosphine ligand, a symmetric 1,5-COD ligand with only one signal observed for the olefinic carbon and hydrogen atoms.

Increasing the reaction ratio of $[(LAu)_3(\mu^3\text{-O})]BF_4$ (L = $PPh_2$-Me, $PPh_2Et$) to (1,5-COD)$PtCl_2$ from 1:1 to 2:1 gives a pale yellow solution. $^{31}$P NMR spectra of the isolated product, $\{(1,5\text{-COD})Pt[\mu^3\text{-O}(AuL)_2]_2\}(BF_4)_2$ (**2**), show a peak slightly upfield of **1**. $^1$H NMR spectra of **2** are almost identical to those of **1**, but integration shows a quadrupling of the phosphine/1,5-

(1) For reviews, see: Bryndza, H. E.; Tam, W. *Chem. Rev.* **1988**, *88*, 1163−1188. Fryzuk, M. D.; Montgomery, C. D. *Coord. Chem. Rev.*, **1989**, *95*, 1−40. Nugent, W. A.; Haymore, B. L. *Coord. Chem. Rev.* **1980**, *31*, 123−175. Also, see: Bennett, M. A.; Jin, H.; Li, S. H.; Rendina, L. M.; Willis, A. C. *J. Am. Chem. Soc.* **1995**, *117*, 8335−8340. Gunguly, S.; Roundhill, D. M. *Organometallics* **1993**, *12*, 4825−4832.

(2) For a discussion of bond energies, see: Bryndza, H. E.; Fong, L. K.; Paciello, R. A.; Tam, W.; Bercaw, J. E. *J. Am. Chem. Soc.* **1987**, *109*, 1444−1456.

(3) Bergman, R. G. *Polyhedron* **1995**, *14*, 3227−3237.

(4) Shan, H.; Yang, Y.; James, A.; Sharp, P. R. *Science* **1997**, *275*, 1460−1462. Ye, C.; Sharp, P. R. *Inorg. Chem.* **1995**, *34*, 55−59. Ge, Y.-W.; Ye, Y.; Sharp, P. R. *J. Am. Chem. Soc.* **1994**, *116*, 8384−8385. Yang, Y.; Sharp, P. R. *J. Am. Chem. Soc.* **1994**, *116*, 6983−6984.

(5) Li, J. J.; Li, W.; Sharp, P. R. *Inorg. Chem.* **1996**, *35*, 604−613.

(6) Shan, H.; Sharp, P. R. *Angew. Chem., Int. Engl. Ed.* **1996**, *35*, 635−636; *Angew. Chem.* **1996**, *108*, 716−717.

(7) Yang, Y.; Sharp, P. R. *Inorg. Chem.* **1993**, *32*, 1946−1951.

(8) For examples, see: Jorgensen, S. W.; Madix, R. J. *J. Am. Chem. Soc.* **1988**, *110*, 397−400. Levis, R. T.; Zhicheng, J.; Winograd, N. *J. Am. Chem. Soc.* **1988**, *110*, 4431−4432. Akhter, S.; White, J. M. *Surf. Sci.* **1986**, *167*, 101−126.

10.1021/ic980818+ CCC: $15.00 
Published on Web 10/15/1998

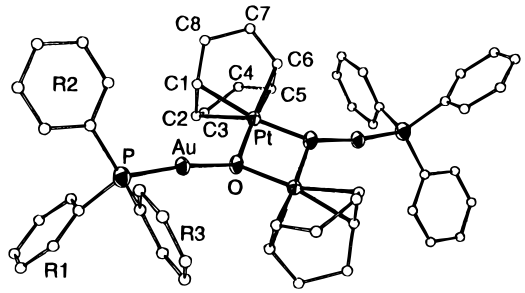


**Figure 1.** ORTEP drawing of the inversion symmetric cationic portion of $[(1,5\text{-COD})Pt(\mu^3\text{-O})(AuPPh_3)]_2(BF_4)_2$ (**1**).

**Scheme 1**

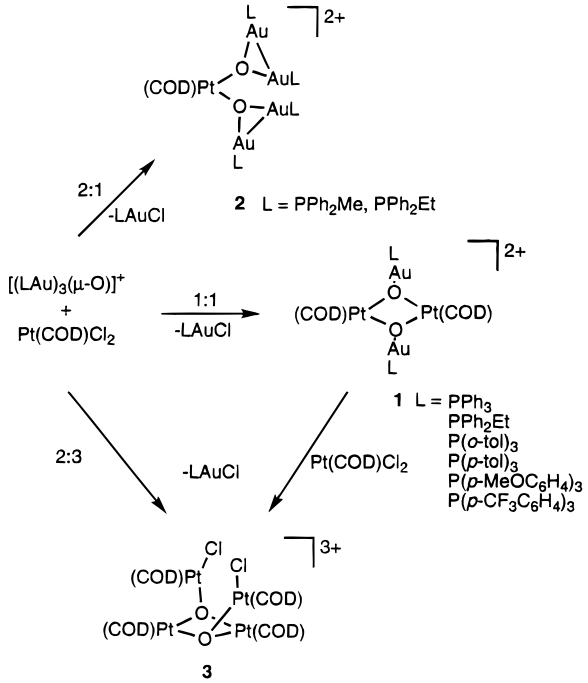


COD ratio. With L = $PPh_2Me$, **2** (L = $PPh_2Me$) is the only product obtained from the reaction of $[(LAu)_3(\mu^3\text{-O})]BF_4$ and (1,5-COD)$PtCl_2$ even with a 1:1 ratio. A proposed structure for **2** is given in Scheme 1. Attempts to grow crystals for an X-ray analysis have failed so far.

Reversing the ratio such that (1,5-COD)$PtCl_2$ is in excess gives LAuCl and a THF-insoluble solid which when dissolved in $CH_2Cl_2$ and precipitated with THF gives pale yellow crystals of $[(1,5\text{-COD})_4Pt_4(\mu^3\text{-O})_2Cl_2](BF_4)_2$ (**3**; Scheme 1). LAuCl is detected in the mother liquor. The structure of **3** was determined by X-ray diffraction, but severe disorder of the solvent molecules ($CH_2Cl_2$) and a large transmission range produced a poor quality structure (see Supporting Information for details). Crystals of the triflate salt $[(1,5\text{-COD})_4Pt_4(\mu^3\text{-O})_2Cl_2](CF_3SO_3)_2$ (**3a**) gave better results, and an ORTEP drawing is given in Figure 2. Crystallographic data are listed in Table 1, and selected distances and angles are presented in Table 3. $^1$H NMR spectra of **3** in $CD_2Cl_2$ show fluxional behavior consistent with rotation of the CODPtCl fragments about the Pt−O bonds. At −60 °C, four olefinic signals in a 1:1:1:1 ratio, consistent with two sets of asymmetric 1,5-COD ligands as observed in the solid-state structure, are observed. The aliphatic region of the $^1$H NMR spectrum is less informative and shows two sets of broad peaks representing the eight different overlapping sets of four methylene protons. As the temperature is raised, two of the olefinic signals (those due to the COD ligands on Pt3 and Pt4 of Figure 2) collapse until at 40 °C, the temperature limit of the solvent, a broad peak overlaid with two sharper peaks (those due to the COD ligands on Pt1 and Pt2 of Figure 2) is observed. $^{13}$C NMR spectra also show fluxional behavior, but a low-temperature limiting spectrum could not be obtained because of the poor solubility of **3**.

The reactions were also investigated with $CH_2Cl_2$ as the reaction solvent. The $^{31}$P NMR spectrum of a mixture of 0.5 equiv of (1,5-COD)$PtCl_2$ and $[(LAu)_3(\mu^3\text{-O})]BF_4$ in $CH_2Cl_2$ shows two broad ($\nu_{1/2}$ = 15 Hz) signals at 34 and 26 ppm. Further addition of (1,5-COD)$PtCl_2$ to the reaction mixture causes the peaks to grow and shift toward each other until they merge to a single broad peak at 28 ppm, suggesting rapid exchange among the species in the reaction mixture. Although LAuCl can be readily isolated from the reactions, in general, only mixtures of Pt containing products are obtained.

When **3** is dissolved in commercially available $CD_2Cl_2$ or $CH_2Cl_2$ which has not been dried or purified, large, colorless, $CH_2Cl_2$-insoluble crystals form on the sides of the container. $^1$H NMR spectra of dissolved crystals in $CD_3NO_2$ show a complex COD pattern. An X-ray analysis of one of the crystals revealed the hydroxo−oxo complex $[(1,5\text{-COD})_4Pt_4(\mu^3\text{-O})_2(\mu^2\text{-OH})](BF_4)_3$ (**4**; Figure 3), evidently formed by hydrolysis of **3**. Crystallographic data are listed in Table 1, and selected distances and angles are presented in Table 4. Attempts to duplicate the hydrolysis by adding water to dried $CH_2Cl_2$ are only partially successful. Colorless crystals are again produced, but they are poorly formed, and $^1$H NMR spectra indicate the presence of other products in addition to **4**. The use of dilute HCl(aq) or dilute $NBu_4OH$(aq) in place of water gave identical results. Further effort will be required to find a reproducible high-yield pathway to **4**.

All of the complexes (**1**−**4**) react readily with $PPh_3$, but only in the case of **1** is the outcome clear. Oxygen transfer from **1** to $PPh_3$ with displacement of COD results in the formation of $[(Ph_3P)_3PtAuPPh_3]BF_4$ (**5**; Scheme 2). **5** is also obtained from the reaction of $Pt(PPh_3)_4$ with $Ph_3PAu^+$. The X-ray crystal structure of this simple "cluster" was determined, and a drawing of the cationic portion is shown in Figure 4. Crystallographic data are given in Table 1, and selected distances and angles are presented in Table 5. The Au atom is linear 2-coordinate bonded to the Pt center and a $Ph_3P$ ligand. The Pt atom is distorted square-planar 4-coordinate and is bonded to two approximately equivalent phosphine ligands cis to the Pt−Au bond and one unique phosphine ligand approximately trans to the Au−Pt bond. All three Pt-bonded phosphine ligands are equivalent by $^{31}$P NMR and are observed as a doublet with $^{195}$Pt satellites. A quartet with $^{195}$Pt satellites is observed for the single Au-bound phosphine. The one-bond P−Pt coupling constant for the Pt-bonded phosphines is the largest (3124 Hz), with the three-bond coupling for the more distant Au-bonded phosphine, as expected, smaller (330 Hz). The observation of only one signal for the Pt-bound phosphine ligands indicates that a fluxional process exchanges the cis and trans ligands. This process probably involves interconversion between a square-planar and a tetrahedral geometry but was not further investigated.

## Discussion

**Reactions.** The oxo/chloro exchange reactions reported here (Scheme 1) and in an earlier communication[6] represent a new entry into late-transition-metal oxo chemistry. We have previously used hydroxo complex deprotonation reactions to prepare late-transition-metal oxo complexes but have found that this

**Table 1.** Crystallographic and Data Collection Parameters

| | **1**·4CDCl$_3$[c] | **3a**·2CH$_2$Cl$_2$ | **4**·CH$_2$Cl$_2$ | **5**·THF |
|---|---|---|---|---|
| formula | $C_{56}H_{58}Au_2B_2Cl_{12}F_8O_2P_2Pt_2$ | $C_{36}H_{52}Cl_6F_6O_8Pt_4S_2$ | $C_{33}H_{51}B_3Cl_2F_{12}O_3Pt_4$ | $C_{76}H_{68}AuBF_4OP_4Pt$ |
| fw | 2208.19 | 1784.00 | 1607.45 | 1600.14 |
| space group | $P\bar{1}$ (No. 2) | $P3_{121}$ (No. 152) | $P2_1/n$ (No. 14) | $P2_1/c$ (No. 14) |
| $T$, °C | −100 | −100 | 22 | 22 |
| $a$, Å | 9.187(4) | 11.8878(4) | 18.624(4) | 20.426(6) |
| $b$, Å | 12.149(3) | 11.8878(4) | 14.760(2) | 13.498(1) |
| $c$, Å | 17.680(6) | 29.3193(15) | 15.584(5) | 24.703(9) |
| α, deg | 99.58(2) | 90 | 90 | 90 |
| $\beta$, deg | 102.86(2) | 90 | 95.538(12) | 97.166(15) |
| $\gamma$, deg | 111.63(2) | 120 | 90 | 90 |
| $V$, Å$^3$ | 1720(1) | 3588.3(3) | 4264(2) | 6758(3) |
| $Z$ | 1 | 3 | 4 | 4 |
| $d_{calc}$, g/cm$^3$ | 2.13 | 2.47 | 2.50 | 1.57 |
| $\lambda$, Å | 0.7093 (Mo) | 0.7107 (Mo) | 0.7093 (Mo) | 0.7093 (Mo) |
| $\mu$, mm$^{-1}$ | 16.9 | 12.2 | 10.0 | 4.37 |
| R1,[a] wR2[b] | 0.025, 0.055 | 0.042, 0.096 | 0.037, 0.048 | 0.034, 0.044 |

[a] $R1 = (\sum||F_o| - |F_c||)/\sum|F_o|$. [b] $wR2 = [(\sum w(|F_o| - |F_c||)^2)/\sum wF_o^2]^{1/2}$ where $w = 4F_o^2/(\sum F_o^2)^2$ for **1**, **4**, and **5**; $wR2 = [(\sum w(F_o^2 - F_c^2)^2)/\sum w(F_c^2)^2]^{1/2}$ with weight $= 1/[\sigma^2(F_o^2) + (0.0459P)^2 + 15.9835P]$; $P = (F_o^2 + 2F_c^2)/3$ for **3a**. [c] Calculations are for the protio form.

**Table 2.** Selected Distances (in Angstroms) and Angles (in Degrees) for [(1,5-COD)Pt($\mu^3$-O)(AuPPh$_3$)]$_2$(BF$_4$)$_2$ (**1**)[a]

| | | | | | |
|---|---|---|---|---|---|
| Pt−O | 2.017(6) | Pt−Oa | 2.007(6) | Au−O | 2.026(6) |
| Au−P | 2.212(3) | Pt−Pta | 3.093(1) | | |
| O−Pt−Oa | 79.5(3) | P−Au−O | 172.4(2) | | |
| Pt−O−Pta | 100.5(3) | Pt−O−Au | 122.8(3) | | |
| Pta-O−Au | 127.3(3) | | | | |

[a] Atoms with an "a" suffix are inversion related to those without the suffix.

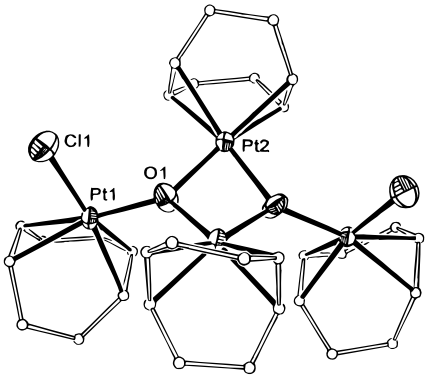


**Figure 2.** ORTEP drawing of the 2-fold symmetric cationic portion of [(1,5-COD)$_4$Pt$_4$($\mu^3$-O)$_2$Cl$_2$](CF$_3$SO$_3$)$_2$ (**3a**).

**Table 3.** Selected Distances (in Angstroms) and Angles (in Degrees) for [(1,5-COD)$_4$Pt$_4$($\mu^3$-O)$_2$Cl$_2$](CF$_3$SO$_3$)$_2$ (**3a**)[a]

| | | | | | |
|---|---|---|---|---|---|
| Pt1−O1 | 1.997(8) | Pt2−O1a | 2.014(7) | Pt2−O1 | 2.022(8) |
| Pt1−Cl1 | 2.304(3) | Pt2−Pt2a | 3.0391(8) | | |
| O1−Pt1−Cl1 | 89.9(3) | O1−Pt2−O1a | 78.0(4) | | |
| Pt1−O1−Pt2a | 129.7(4) | Pt1−O1−Pt2 | 131.1(4) | | |
| Pt2−O1−Pt2a | 97.7(3) | | | | |

[a] Atoms with an "a" suffix are 2-fold related to those without the suffix.

route cannot be applied to (1,5-COD)Pt complexes. We have been unable to prepare the requisite hydroxo complex [(1,5-COD)Pt($\mu^2$-OH)]$_2^{2+}$ even though analogous Rh and Ir complexes are known.[9−11] The exchange reaction is currently the only route into (1,5-COD)Pt oxo chemistry. Unfortunately, the reactions are limited. Attempts to prepare the norbornadiene and tetrafluorobarrelene analogues of **1**−**3** have failed so far.

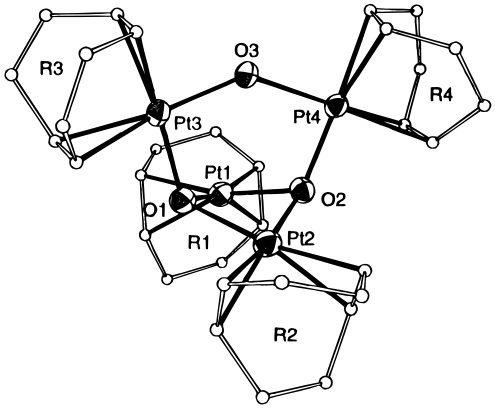


**Figure 3.** ORTEP drawing of the cationic portion of [(1,5-COD)$_4$Pt$_4$-($\mu^3$-O)$_2$($\mu^2$-OH)](BF$_4$)$_3$ (**4**).

**Table 4.** Selected Distances (in Angstroms) and Angles (in Degrees) for [(1,5-COD)$_4$Pt$_4$($\mu^3$-O)$_2$($\mu^2$-OH)](BF$_4$)$_3$ (**4**)

| | | | | | |
|---|---|---|---|---|---|
| Pt1−O1 | 2.012(8) | Pt1−O2 | 2.014(9) | Pt2−O1 | 2.060(8) |
| Pt2−O2 | 2.032(8) | Pt3−O1 | 2.029(8) | Pt3−O3 | 2.062(8) |
| Pt4−O2 | 2.016(8) | Pt4−O3 | 2.052(8) | | |
| O1−Pt1−O2 | 81.4(3) | O1−Pt2−O2 | 79.8(3) | | |
| O1−Pt3−O3 | 92.8(3) | O2−Pt4−O3 | 91.5(3) | | |
| Pt1−O1−Pt | 291.9(3) | Pt1−O1−Pt3 | 115.1(4) | | |
| Pt2−O1−Pt3 | 114.6(4) | Pt1−O2−Pt2 | 92.7(3) | | |
| Pt1−O2−Pt4 | 118.9(4) | Pt2−O2−Pt4 | 113.5(4) | | |
| Pt3−O3−Pt4 | 138.1(4) | | | | |

(We also have attempted imido/chloro and nitrido/chloro exchange reactions using [(LAu)$_3$($\mu$-NR)]BF$_4$ and [(LAu)$_4$($\mu$-N)]BF$_4$ with only limited success.) This may be due to the equilibrium nature of the reactions as revealed by the $^{31}$P NMR studies of mixtures of [(LAu)$_3$($\mu^3$-O)]BF$_4$ and (1,5-COD)PtCl$_2$ in CH$_2$Cl$_2$. In this solvent, all species are soluble and give exchange-broadened peaks. Successful isolation of pure products is only possible when factors favor a particular species (e.g., the insolubility of **3** in THF). Equilibria must be considered in successful applications of the exchange chemistry to other systems.

(9) Uson, R.; Oro, L. A.; Cabeza, J. A. *Inorg. Synth.* **1985**, *23*, 126−130 and references therein.

(10) Selent, D.; Ramn, M. *J. Organomet. Chem.* **1995**, *485*, 135. Ramn, M.; Selent, D. *Acta Crystallogr., Sect. C* **1996**, *52*, 2703. Krzyzanowski, P.; Kubicki, M.; Marciniec, B. *Polyhedron* **1996**, *15*, 1. Vizi-Orosz, A.; Ugo, R.; Psaro, R.; Sironi, A.; Moret, M.; Zucchi, C.; Ghelfi, F.; Palyi, G. *Inorg. Chem.* **1994**, *33*, 4600.

(11) Tanaka, I.; Jin-No, N.; Kushida, T.; Tsutsui, N.; Ashida, T.; Suzuki, H.; Sakurai, H.; Moro-Oka, Y.; Ikawa, T. *Bull. Chem. Soc. Jpn.* **1983**, *56*, 657.

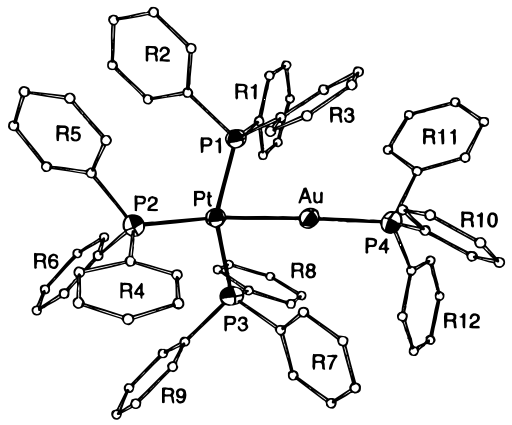


**Figure 4.** ORTEP drawing of the cationic portion of $[(Ph_3P)_3PtAuPPh_3]BF_4$ (**5**).

**Scheme 2**

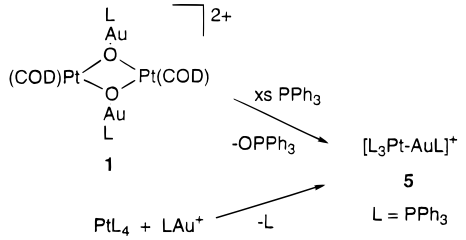


**Table 5.** Selected Distances (in Angstroms) and Angles (in Degrees) for $[(Ph_3P)_3PtAuPPh_3]BF_4$ (**5**)

| | | | | | |
|---|---|---|---|---|---|
| Pt−Au | 2.6158(7) | Pt−P1 | 2.270(2) | Pt−P2 | 2.348(2) |
| Pt−P3 | 2.308(2) | Au−P4 | 2.288(2) | | |

| | | | |
|---|---|---|---|
| Au−Pt−P1 | 75.74(5) | Au−Pt−P2 | 168.26(6) |
| Au−Pt−P3 | 76.52(6) | P1−Pt−P2 | 109.55(8) |
| P1−Pt−P3 | 149.79(8) | P2−Pt−P3 | 99.97(8) |
| Pt−Au−P4 | 171.13(6) | | |

Considering the "pseudo-proton" nature of $LAu^+$,[12] **1** and **2** may be viewed as aura−hydroxo ($OAuL^-$) and aura−aqua $[O(AuL)_2]$ complexes. Analogous Pt hydroxo and aqua complexes, $[L_2Pt(\mu\text{-}OH)]_2^{2+}$ and $L_2Pt(OH_2)_2^{2+}$,[5,13] are well-known, although not for $L_2$ = 1,5-COD. Similarly, our previously reported complexes $\{(diene)M[\mu^4\text{-}O(AuPPh_3)_2]\}_2(BF_4)_2$ (M = Rh, Ir; diene = 1,5-COD, NBD)[6] are bridging aura−aqua complexes. The addition of $LAu^+$ to **1** (L = $PPh_3$) was explored with the idea of generating an analogous Pt aura−aqua bridged complex. Although $^{31}P$ NMR spectroscopy showed only a single broad peak for mixtures of **1** and $LAu^+$ (generated in situ from LAuCl and $AgBF_4$), only **1** could be isolated.

The formation and stability of **3** is surprising. We had expected that further reaction of **1** with (1,5-COD)$PtCl_2$ would result in the replacement of the two oxo-bonded $LAu^+$ fragments with a single (1,5-COD)$Pt^{2+}$ fragment, giving trinuclear $[\{(1,5\text{-}COD)Pt\}_3(\mu^3\text{-}O)_2]^{2+}$ and LAuCl. Analogous $[(L_2Pt)_3(\mu^3\text{-}O)_2]^{2+}$ (L = $PMe_2Ph$)[5] and $[(L_2Pt)_2(1,5\text{-}COD)Rh(\mu^3\text{-}O)_2]^+$ (L = $PPh_3$)[14] are known stable complexes. Complex **3** could form $\{[(1,5\text{-}COD)Pt]_3(\mu^3\text{-}O)_2\}^{2+}$ by elimination of (1,5-COD)$PtCl_2$, a process that should be entropically favored and would result in no loss of Pt−Cl or Pt−O bonds, but shows no tendency to do so.

A common feature of 1,5-COD metal chemistry is substitution. The 1,5-COD ligand is often readily displaced by phosphines or CO, yielding phosphine or CO analogues of the COD complex. Simple substitution is not observed with **1**−**4**. Degradation of the structures occurs with CO or $PPh_3$. The formation of $OPPh_3$ in the $PPh_3$ reactions indicates that COD ligand displacement is accompanied by oxygen-atom transfer.[15] No intermediates are detected even with a deficiency of $PPh_3$, suggesting that the oxygen-atom transfer reaction occurs at least as rapidly as the 1,5-COD displacement from the Pt center. It is possible that the expected $PPh_3$ oxo complexes are more reactive than the COD oxo complexes. However, the expected $PPh_3$ oxo complex from **1**, $[(Ph_3P)_2Pt(\mu^2\text{-}O)]_2$ (assuming $LAu^+$ and 1,5-COD displacement), is known and only slowly oxidizes $PPh_3$.[16]

**Structures.** The structures may be analyzed using the isolobal relationship of $LAu^+$ and $R^+$ (R = H, alkyl, etc.).[12] Complex **1** is then analogous to $[(1,5\text{-}COD)Pt(\mu^2\text{-}OR)]_2^{2+}$. This class of complex is unknown for Pt, but isoelectronic $[(1,5\text{-}COD)M(\mu^2\text{-}OR)]_2$ complexes (M = Rh, Ir) are known, and several of the Rh derivatives have been structurally characterized. Only the R = Me derivative[11] has a planar core structure like that of **1**. Other derivatives (R = H, Et, $SiMe_3$, $SiPh_3$)[9] have nonplanar structures folded at the O-atom bridges, giving short Rh−Rh distances.[17] Comparisons with **1** will be restricted to the planar derivative $[(1,5\text{-}COD)Rh(\mu^2\text{-}OMe)]_2$. The $M_2O_2$ cores of **1** and $[(1,5\text{-}COD)Rh(\mu^2\text{-}OMe)]_2$ are very similar. The O−M−O angles are 76.5° (Rh) and 79.5(3)° (**1**), and the M−O−M angles are 103.5° (Rh) and 100.5(3)° (**1**). The average M−O bond distances show that the Pt−O distance of **1** {2.012(7) Å} is significantly shorter than the Rh−O distance (2.057 Å). Given the greater covalent radius of Pt, a longer Pt−O distance is expected. A comparison of the average Rh−C (2.092 Å) and Pt−C (2.144 Å) distances in the two structures is consistent with a smaller Rh radius. In related $[L_2Pt(\mu^2\text{-}OH)]_2^{2+}$ (L = a phosphine), the average Pt−O distances are also greater than that in **1**, ranging from 2.03 to 2.08 Å.[5]

$[(C_8H_{12}OMe)Pt(\mu^2\text{-}OMe)]_2$,[18] the formal $MeO^-$ addition product of unknown $[(1,5\text{-}COD)Pt(\mu^2\text{-}OMe)]_2^{2+}$, may also be

(12) Hall, K. P.; Mingos, D. M. P. *Prog. Inorg. Chem.* **1984**, *32*, 237−325. Evans, D. G.; Mingos, D. M. P. *J. Organomet. Chem.* **1982**, *232*, 171−191.

(13) Fallis, S.; Anderson, G. K.; Rath, N. P. *Organometallics* **1991**, *10*, 3180−3184. Stang, P. J.; Olenyuk, B.; Fan, J.; Arif, A. M. *Organometallics* **1996**, *15*, 904−908. Siegmann, K.; Pregosin, P. S.; Venanzi, L. M. *Organometallics* **1989**, *8*, 2659. Bandini, A. L.; Banditelli, G.; Demartin, F.; Manaserro, M.; Minghetti, G. *Gazz. Chim. Ital.* **1993**, *123*, 417−423. Bushnell, G. W.; Dixon, K. R.; Hunter, R. G.; McFarland, J. J. *Can. J. Chem.* **1972**, *50*, 3694. Bushnell, G. W. *Can. J. Chem.* **1978**, *56*, 1773. Wimmer, S.; Castan, P.; Wimmer, F. L.; Johnson, N. P. *J. Chem. Soc., Dalton Trans.* **1989**, 403−412. Trovo, G.; Bandoli, G.; Casellato, U.; Corain, B.; Nicolini, M.; Longata, B. *Inorg. Chem.* **1990**, *29*, 4616−4621. Scarcia, V.; Furlani, A.; Longato, B.; Corain, B. *Inorg. Chim. Acta* **1988**, *153*, 67−70. Longata, B.; Pilloni, G.; Valle, G.; Corain, B. *Inorg. Chem.* **1988**, *27*, 956. Miyamoto, T. K. *Chem. Lett.* **1994**, 1971. Rochon, F. D.; Melanson, R.; Morneau, A. *Magn. Reson. Chem.* **1992**, *30*, 697. Ericson, V.; Lovqvist, K.; Noren, B.; Oskarsson, A. *Acta Chem. Scand.* **1992**, *46*, 854. Rochon, F. D.; Kong, P. C.; Melanson, R. *Acta Crystallogr., Sect. C* **1985**, *41*, 1602. Rochon, F. D.; Guay, F. *Acta Crystallogr., Sect. C* **1987**, *43*, 43.

(14) Li, W. Ph.D. Thesis, University of Missouri, Columbia, 1993.

(15) For other examples of phosphine oxidation by late-transition-metal oxo complexes, see: Brownlee, G. S.; Carty, P.; Cash, D. N.; Walker, A. *Inorg. Chem.* **1975**, *14*, 323−327. McGhee, W. D.; Foo, T.; Hollander, F. J.; Bergman, R. G. *J. Am. Chem. Soc.* **1988**, *110*, 8543. Dobbs, D. A.; Bergman, R. G. *Organometallics* **1994**, *13*, 4594−4605. Also, see ref 16.

(16) Li, W.; Barnes, C. L.; Sharp, P. R. *J. Chem. Soc., Chem. Commun.* **1990**, 1634−1636.

(17) Theoretical studies indicate a soft potential for folding in this type of dimer, and small perturbations can give bent or planar geometries. For example, see: Summerville, R. H.; Hoffmann, R. *J. Am. Chem. Soc.* **1976**, *98*, 7240. Also, see: Aullon, G.; Ujaque, G.; Lledos, A.; Alvarez, S.; Alemany, P. *Inorg. Chem.* **1998**, *37*, 804−813.

(18) Giordano, F.; Vitagliano, A. *Inorg. Chem.* **1981**, *20*, 633.

compared to **1**. There are two different Pt−O bond distances in this complex. The distance trans to the coordinated double bond is the shortest at 2.04 Å but is still longer than that in **1**. These comparisons suggest that the Pt−O bond is shorter in **1** than would be expected for an analogous OR complex. We have previously noted a slight shortening of the Pt−O bond distance on deprotonation of hydroxo complexes.[5] The Au−O distance of 2.026 Å in **1** is typical of the Au−O bond distances found in $[(LAu)_3(\mu^3\text{-O})]^+$ (L = a phosphine).[7,19]

Complex **3a** is analogous to **1** where the two $LAu^+$ fragments have been replaced with two (1,5-COD)ClPt$^+$ fragments. The $Pt_2O_2$ "diamond" core of **1** is planar whereas it is folded (28.7°) at the O−O hinge in **3a**. The Pt−O bond distances [2.018(6) Å] in the $Pt_2O_2$ core of **3a** are identical to those in **1**. However, the folding in **3a** results in a significant decrease in the average Pt−O−Pt core angles from 100.5(3)° in **1** to 97.7(3)° in **3**. A larger folding of 38° is observed in the structure of **4**, and as in **2**, this is accompanied by a reduced average Pt−O−Pt core angle of 92.7(3)°. The average Pt−O distance in the $Pt_2O_2$ core of **4** [2.030(22) Å] appears longer than that in **1** but shows considerable variation, ranging from 2.012(8) to 2.060(8) Å.

An internal comparison of hydroxo- and oxo-ligand bond distances is possible in **4**. The average Pt−O bond distance involving the hydroxo ligand is 2.057(7) Å whereas that of the oxo ligands is at 2.027(18) Å. Again, variations in the oxo-ligand distances makes comparison difficult. In addition, the different coordination environment of the hydroxo ligand may contribute to the difficulty of this comparison. The Pt3−O3−Pt4 angle of the hydroxo bridge of **4** is remarkably large [138.1(4)°] and may represent a strained situation. The structure of **4** may also be considered to derive from a heterocubane structure where one oxygen atom has been removed and one of the Pt−O bonds (OH) has been broken. Heterocubane structures are common in early-transition-metal oxo chemistry.[20]

$[(Ph_3P)_3PtAuPPh_3]^+$ **5** is analogous to the hydride complexes $[L_3PtH]^+$ (L = a phosphine). Several hydride complexes of this type have been structurally characterized[21] and have structures closely related to that of **5**. The hydride ligand was not located, restricting comparisons to the Pt−P metrical parameters. As with **5**, distorted square-planar geometries are observed. The three P−Pt−P angles group into two sets. The angles between the trans phosphorus atoms range from 154° to 160° whereas the cis angles range from 99° to 107°. The trans phosphorus-atom angle in **5** is 150° whereas the two cis angles are 100° and 110°, indicating somewhat greater distortion from square-planar geometry for **5**. The hydride complexes show an elongation of the trans-to-hydride Pt−P bond relative to the cis-to-hydride Pt−P bonds. The average distance difference ranges from 0.033 to 0.050 Å and reflects the strong trans influence[22] of the hydride ligand. The corresponding distance difference in **5**, the difference between the average cis-to-Au Pt−P distance and the trans-to-Au distance, is 0.059 Å, suggesting a greater trans influence for LAu over H.

## Conclusions

Oxo/chloro exchange reactions using $[(LAu)_3(\mu^3\text{-O})]^+$ (L = a phosphine) as the oxo source have provided a unique entry into (1,5-COD)Pt oxo chemistry. The resulting oxo complexes display intriguing structures involving oxo ligands bridging between Pt and Au centers. The Pt/Au oxo complexes may be regarded as aura−hydroxo and aura−aqua complexes of Pt(II). The oxo group dominates the reaction chemistry of the complexes, and simple 1,5-COD substitution chemistry is not observed. Structural data on the complexes support shorter M−O distances in oxo complexes as compared to those in analogous hydroxo and alkoxo complexes.

## Experimental Section

**General Procedures.** Experiments were routinely performed under a dinitrogen atmosphere in a Vacuum Atmospheres Co. drybox or by Schlenk techniques. Solvents were dried by standard techniques and were stored under dinitrogen over 4 Å molecular sieves except where indicated. Reagents were purchased from Aldrich Chemicals and were used as received. Deuterated solvents were obtained from Cambridge Isotope Laboratories and were dried over activated alumina. (1,5-COD)$PtCl_2$,[23] $[(LAu)_3(\mu^3\text{-O})]BF_4$,[7,19] and $Pt(PPh_3)_4$[24] were synthesized according to literature procedures. NMR spectra were recorded on Bruker AMX-500 or AMX-250 spectrometers. $^1$H NMR spectra are referenced to TMS or to protic solvent impurities referenced back to TMS. $^{31}$P NMR spectra are referenced to external 85% $H_3PO_4$. $^{195}$Pt NMR spectra are referenced to external $K_2PtCl_6$(aq). All NMR shifts are in ppm with negative shifts upfield from the reference. Infrared spectra (frequencies given in cm$^{-1}$) were recorded on a Nicolet 550 Magna FTIR spectrometer using NaCl plates. Spectra were recorded at ambient temperatures (22 °C) unless otherwise indicated. Desert Analytics or National Chemical Consulting performed the microanalyses (inert atmosphere).

**$[(1,5\text{-COD})Pt(\mu^3\text{-O})(AuPPh_3)]_2(BF_4)_2$ (1; L = $PPh_3$).** A solution of Pt(1,5-COD)$Cl_2$ (74.8 mg, 0.200 mmol) in THF (50 mL) was vigorously stirred with solid $[(LAu)_3(\mu^3\text{-O})]BF_4$ (296 mg, 0.200 mmol). The mixture became yellow within 30 min. Stirring was continued for 2 h. Half of the solvent was then removed in vacuo, followed by the addition of 50 mL of ether. The resulting pale orange-yellow microcrystalline solid was isolated by filtration, recrystallized from $CH_2Cl_2$/ether, and dried in vacuo. Yield: 170 mg (99%). Anal. Calcd (found) for $C_{52}H_{54}Au_2B_2F_8O_2P_2Pt_2$: C, 36.09 (35.76); H, 3.15 (3.32). Crystals for X-ray analysis were obtained from $CDCl_3$. $^1$H NMR (250 MHz, $CD_2Cl_2$): 7.42−7.67 (m, 15H, Ph), 5.23 (br, 4H, CH, weak satellites observed, $J_{Pt-H}$ = 58.8 Hz), 2.78 (br, 4H, $CH_2$), 2.29 (d of t, 4H, $CH_2$, $J_{H-H}$ = 8.5 Hz, $J'_{H-H}$ = 7.5 Hz). $^{13}$C{$^1$H} NMR (125.8 MHz, $CDCl_3$): 134.20 (d, *o*-Ph, $J_{P-C}$ = 13.2 Hz), 133.01 (s, *p*-Ph), 129.94 (d, *m*-Ph, $J_{P-C}$ = 12.1 Hz), 127.53 (d, *i*-Ph, $J_{P-C}$ = 68 Hz), 97.18 (s, CH, no satellites observed), 30.46 (s, $CH_2$). $^{31}$P{$^1$H} NMR (101.3 MHz, $CH_2Cl_2$): 26.6 (s). $^{195}$Pt NMR (64.5 MHz, $CD_2Cl_2$): −2512 (s). IR (thin film): 3050−2848 (m, C−H), 1480, 1436 (m, C═C), 1056 (br, s, B−F).

**L = $PPh_2$-*i*-Pr.** The same procedure as that for L = $PPh_3$ was used. Yield: 78%. $^1$H NMR (250 MHz, $CDCl_3$): 7.68−7.46 (m, 10H, Ph), 5.23 (br, 4H, CH, no satellites observed), 2.87 (d sept, overlapped with the COD−$CH_2$, 1H, C*H*$Me_2$), 2.83 (br, 4H, $CH_2$), 2.18 (br, 4H, $CH_2$), 1.13 (dd, $J_{HH}$ = 6.8 Hz, $J_{HP}$ = 20.0 Hz, 6H, CH*Me*$_2$). $^{31}$P{$^1$H} NMR (101.3 MHz, $CDCl_3$): 41.7 (s).

**L = $PPh_2$Et.** The same procedure as that for L = $PPh_3$ was used. Yield: 74%. Anal. Calcd (found) for $C_{44}H_{54}Au_2B_2F_8O_2P_2Pt_2$: C, 32.33 (32.50); H, 3.33 (3.14). $^1$H NMR (250 MHz, $CDCl_3$): 7.62−7.44 (m, 10H, Ph), 5.17 (br, 4H, CH, no satellites observed), 2.74 (br, 4H, $CH_2$),

(19) Nesmeyanov, A. N.; Perevalova, E. G.; Struchkov, Y. T.; Antipin, M. Y.; Grandberg, K. I.; Dyadchenko, V. P. *J. Organomet. Chem.* **1980**, *201*, 343−349. Kolb, A.; Bissinger, P.; Schmidbaur, H. *Z. Anorg. Allg. Chem.* **1993**, *619*, 1580.
(20) West, B. O. *Polyhedron* **1989**, *8*, 219−274. Bottomley, F.; Sutin, L. *Adv. Organomet. Chem.* **1988**, *28*, 339.
(21) Manojlovic-Muir, L.; Jobe, I. R.; Ling, S. S. M.; McLennan, A. J.; Puddephatt, R. J. *J. Chem. Soc., Chem. Commun*. **1985**, 1725. Caputo, R. E.; Mak, D. K.; Willett, R. D.; Roundhill, S. G. N.; Roundhill, D. M. *Acta Crystallogr., Sect. B* **1977**, *33*, 215. Packett, D. L.; Syed, A.; Trogler, W. C. *Organometallics* **1988**, *7*, 159. Russell, D. R.; Mazid, M. A.; Tucker, P. A. *J. Chem. Soc., Dalton Trans.* **1980**, 1737.
(22) Appleton, T. G.; Clark, H. C.; Manzer, L. E. *Coord. Chem. Rev.* **1973**, *10*, 335−422.
(23) McDermott, J. X.; White, J. F.; Whitesides, G. M. *J. Am. Chem. Soc.* **1976**, *98*, 6521.
(24) Ugo, R.; Cariati, F.; La Monica, G. *Inorg. Synth.* **1990**, *28*, 123.

2.47 (dq, $J_{HH}$ = 7.4 Hz, $J_{HP}$ = 10.4 Hz, 2H, C$H_2$Me), 2.17 (br, 4H, $CH_2$), 1.14 (dt, $J_{HH}$ = 7.4 Hz, $J_{HP}$ = 23.0 Hz, 3H, $CH_2$*Me*). $^{31}P\{^1H\}$ NMR (101.3 MHz, $CDCl_3$): 27.1 (s).

**L = P(*o*-tol)$_3$.** The same procedure as that for L = $PPh_3$ was used. Yield: 79%. $^1H$ NMR (250 MHz, $CDCl_3$): 7.56−6.93 (m, 12H, Ph), 5.05 (br, 4H, CH, no satellites observed), 2.63 (br, 4H, $CH_2$), 2.61 (s, 9H, Me), 2.13 (br, 4H, $CH_2$). $^{31}P\{^1H\}$ NMR (101.3 MHz, $CDCl_3$): 3.3 (s).

**L = P(*p*-tol)$_3$.** The same procedure as that for L = $PPh_3$ was used. Yield: 84%. Anal. Calcd (found) for $C_{58}H_{66}Au_2B_2F_8O_2P_2Pt_2$: C, 38.39 (38.63); H, 3.67 (3.85). $^1H$ NMR (250 MHz, $CDCl_3$): 7.40−7.24 (m, 12H, Ph), 5.19 (br, 4H, CH, no satellites observed), 2.79 (br, 4H, $CH_2$), 2.40 (s, 9H, Me), 2.20 (br, 4H, $CH_2$). $^{31}P\{^1H\}$ NMR (101.3 MHz, $CDCl_3$): 24.0 (s).

**L = P(*p*-MeOC$_6$H$_4$)$_3$.** The same procedure as that for L = $PPh_3$ was used. Yield: 84%. Anal. Calcd (found) for $C_{58}H_{66}Au_2B_2F_8O_8P_2Pt_2$: C, 36.46 (36.24); H, 3.48 (3.11). $^1H$ NMR (250 MHz, $CDCl_3$): 7.38−7.01 (m, 12H, Ph), 5.20 (br, 4H, CH, no satellites observed), 3.85 (s, 9H, OMe), 2.82 (br, 4H, $CH_2$), 2.21 (br, 4H, $CH_2$). $^{31}P\{^1H\}$ NMR (101.3 MHz, $CDCl_3$): 22.0 (s).

**L = P(*p*-CF$_3$C$_6$H$_4$)$_3$.** The same procedure as that for L = $PPh_3$ was used. Yield: 83%. $^1H$ NMR (250 MHz, $CDCl_3$): 7.84−7.62 (m, 12H, Ph), 5.22 (br, 4H, CH, no satellites observed), 2.80 (br, 4H, $CH_2$), 2.10 (br, 4H, $CH_2$). $^{31}P\{^1H\}$ NMR (101.3 MHz, $CDCl_3$): 25.9 (s).

**[(1,5-COD)Pt{$\mu^3$-O(AuL)$_2$}$_2$](BF$_4$)$_2$ (2; L = PPh$_2$Et).** A solution of Pt(COD)$Cl_2$ (18 mg, 0.05 mmol) in THF (8 mL) was vigorously stirred with solid [(LAu)$_3$($\mu^3$-O)]$BF_4$ (134 mg, 0.10 mmol). The mixture became an almost clear pale yellow solution in 2 h. Half of the solvent was then removed in vacuo, followed by the addition of 15 mL of ether. The resulting light yellow solid was isolated by filtration, recrystallized from $CH_2Cl_2$/ether, and dried in vacuo. Yield: 50 mg (73%). Anal. Calcd (found) for $C_{64}H_{72}Au_4B_2F_8O_2P_4Pt$: C, 35.69 (35.28); H, 3.37 (3.06). $^1H$ NMR (250 MHz, $CDCl_3$): 7.65−7.38 (m, 40H, Ph), 5.18 (br, 4H, CH, no satellites observed), 2.74 (br, 4H, $CH_2$), 2.49 (dq, $J_{HH}$ = 7.4 Hz, $J_{HP}$ = 10.4 Hz, 8H, C$H_2$Me), 2.17 (br, 4H, $CH_2$), 1.14 (dt, $J_{HH}$ = 7.3 Hz, $J_{HP}$ = 23.0 Hz, 12H, $CH_2$*Me*). $^{31}P\{^1H\}$ NMR (101.3 MHz, $CDCl_3$): 25.9 (s).

**L = PPh$_2$Me.** The same procedure as that for L = $PPh_2Et$ was used. Yield: 75%. Anal. Calcd (found) for $C_{60}H_{64}Au_4B_2F_8O_2P_4Pt$: C, 34.36 (34.60); H, 3.08 (2.93). $^1H$ NMR (250 MHz, $CDCl_3$): 7.57−7.35 (m, 40H, Ph), 5.25 (br, 4H, CH, no satellites observed), 2.73 (br, 4H, $CH_2$), 2.19 (br, 4H, $CH_2$), 2.06 (d, $J_{HP}$ = 8.0 Hz, 12H, Me). $^{31}P\{^1H\}$ NMR (101.3 MHz, $CDCl_3$): 10.3 (s).

**[(1,5-COD)$_4$Pt$_4$($\mu^3$-O)$_2$Cl$_2$](BF$_4$)$_2$ (3).** A solution of [($Ph_3PAu$)$_3$($\mu^3$-O)]$BF_4$ (148 mg, 0.100 mmol) in $CH_2Cl_2$ (1 mL) was added dropwise to a stirred suspension of Pt(1,5-COD)$Cl_2$ (75 mg, 0.20 mmol) in THF (10 mL). The mixture became pale yellow within 30 min. Stirring was continued for 2 h. The resulting pale yellow solid (108 mg) was isolated by filtration, washed with THF and ether, and dried in vacuo. The solid was dissolved in a minimum volume of $CH_2Cl_2$ (∼5 mL), and the solution was filtered, layered with THF (∼13 mL), and stored at −30 °C for 12 h. Pale yellow feathery needle crystals of **3** were isolated by filtration, washed with ether, and dried in vacuo. Yield: 56 mg (75%). Anal. Calcd (found) for $C_{32}H_{48}B_2Cl_2F_8O_2Pt_4\cdot CH_2Cl_2$: C, 25.17 (25.18); H, 3.20 (3.14). (NMR spectroscopy and X-ray analysis confirm the presence of $CH_2Cl_2$.) Crystals for X-ray analysis were obtained by cooling of a saturated $CD_2Cl_2$ solution of the complex. The $CF_3SO_3^-$ salt (**3a**) was prepared by an analogous procedure using [($Ph_3PAu$)$_3$($\mu^3$-O)][$CF_3SO_3$] and toluene in place of THF. Crystals for X-ray analysis were obtained by cooling of a toluene-layered $CH_2Cl_2$ solution of the complex. $^1H$ NMR (300 MHz, $CD_2Cl_2$, −70 °C): 5.95 (br s, no satellite peaks observed, 4H, CH of COD on PtCl), 5.77 (br s, no satellite peaks observed, 4H, CH of COD on $Pt_2O_2$), 5.52 (br s, no satellite peaks observed, 4H, CH of COD on $Pt_2O_2$), 5.37 (br s, no satellite peaks observed, 4H, CH of COD on $Pt_2O_2$), 2.8 and 2.6 (br m, 16H, $CH_2$), 2.2 (br m, 16H, $CH_2$). At 37 °C: 5.84 (br s, no satellite peaks observed, 4H, CH of COD on $Pt_2O_2$), 5.8 (v br s, $\nu_{1/2} \approx$ 120 Hz, average CH of COD on PtCl), 5.44 (br s, no satellite peaks observed, 4H, CH of COD on $Pt_2O_2$), 2.8 and 2.6 (br m, 16H, $CH_2$), 2.2 (br m, 16H, $CH_2$). Small peaks due to a persistent unidentified species are observed at 5.88, 5.45, and 4.79 ppm. $^{13}C\{^1H\}$ NMR (126 MHz, $CD_2Cl_2$): 100.90 (s with satellites, CH of COD on $Pt_2O_2$, $J_{Pt-H}$ = 76 Hz), 31.24 (s, $CH_2$ of COD on $Pt_2O_2$), 30.47 (s, $CH_2$ of COD on $Pt_2O_2$), 30.4 (br s, $CH_2$ of COD on PtCl). A slight rise in the baseline is detected at ca. 98 ppm and probably represents the exchanging olefinic signals of the CODPtCl fragment. The low solubility of **3** precluded low-temperature carbon NMR.

**[(Ph$_3$P)$_3$PtAuPPh$_3$]BF$_4$ (5). From 1 and PPh$_3$.** A solution of $PPh_3$ (42 mg, 0.16 mmol) in THF (3 mL) was stirred vigorously with solid **1** (34 mg, 0.020 mmol). The mixture became a clear orange-yellow solution within 10 min. Stirring was continued for 15 min. Addition of 15 mL of $Et_2O$ to the reaction mixture gave the product as a yellow precipitate, which was filtered off, washed with $Et_2O$, and dried in vacuo. Yield: 55 mg (90%). Crystals for X-ray analysis were obtained from concentrated THF solutions. **5** is not sensitive to air and moisture but readily decomposes in chlorinated solvents, yielding ($PPh_3$)$_2PtCl_2$ and ($PPh_3$)$_2Au^+$.

**From (Ph$_3$P)$_4$Pt and Ph$_3$PAu$^+$.** A solution of $Ph_3PAuBF_4$ (generated in situ from 50 mg of $Ph_3PAuCl$ and 19 mg of $AgBF_4$, 0.10 mmol) in THF (5 mL) was stirred vigorously with solid Pt($PPh_3$)$_4$ (124 mg, 0.10 mmol). After 10 min, 15 mL of $Et_2O$ was added to the deep yellow reaction mixture to precipitate the yellow product. The product was filtered off, washed with $Et_2O$, and dried in vacuo. Yield: 135 mg (88%). Anal. Calcd (found) for $C_{72}H_{60}AuBF_4P_4Pt$: C, 56.60 (56.23); H, 3.96 (3.33). $^{31}P$ NMR (200 MHz, THF): 34.0 (d with satellites, 3P, $^3J_{PP}$ = 60 Hz, $^1J_{PtP}$ = 3124 Hz), 36.8 (q with satellites, 1P, $^3J_{PP}$ = 60 Hz, $^2J_{PtP}$ = 330 Hz).

**Crystal Structure Analyses.** Crystal data, reflection collection and processing parameters, and solution and refinement data are summarized in abbreviated Table 1. A full description (CIF format) is given in the Supporting Information. Crystals were grown as described in the synthesis section above. Those done at low temperature were mounted by transferring the crystals from the mother liquor into a pool of heavy oil. A suitable crystal was selected and removed from the oil with a glass fiber. With the oil-covered crystal adhering to the end of the glass fiber, the sample was transferred to an $N_2$ cold stream on the diffractometer and data collection begun. Those done at ambient temperatures were glued with epoxy to the end of a glass fiber and coated with epoxy. Data collection and analysis followed routine procedures.

**Acknowledgment.** We thank the Division of Chemical Sciences, Office of Basic Energy Sciences, Office of Energy Research, U.S. Department of Energy (Grant No. DF-FG02-88ER13880), for support of this work. Grants from the National Science Foundation provided a portion of the funds for the purchase of X-ray (CHE-9011804) and NMR (PCM-8115599 and CHE 89-08304) equipment.

**Supporting Information Available:** X-ray crystallographic files for **1**, **3**, **3a**, **4**, and **5** in CIF format are available on the Internet only. Access information is given on any current masthead page.

IC980818+